Chapter 8
Advances in Neuroimaging Techniques with PET

Eku Shimosegawa

Abstract Using a radioisotope, positron emission tomography (PET) can obtain images of natural circulation through the body (from blood vessels to organs and from organs to blood vessels) as molecular images, which is naturally present *in vivo*. A distinctive feature of PET molecular imaging is to use radioisotope compounds as tracers. This chapter describes the latest status of imaging research on neurological functions, to the extent to which they are related to PET. Although PET has limitations, e.g., on spatial resolution, radiation exposure and observation period due to short half-life isotopes, it can visually and dynamically evaluate normal brain function and pathophysiology. Newly-developed imaging devices (e.g., semiconductor PET and PET/MR), in combination with improved imaging techniques and innovative analytical procedures, are expected to be powerful tools for studying the brain function in detail.

Keywords PET • Energy metabolism • CBF • Semiconductor PET • PET/MR

8.1 Introduction

In vivo imaging is largely classified into morphological, functional and molecular imaging. Morphological imaging represents spatial information, such as intraorgan structure and vasculature, based on anatomy, while functional imaging physiologically and biochemically visualizes circulation at the tissue level and intracellular changes. Molecular imaging visualizes the functions and dynamics of biofunctional molecules based on molecular biology. Specifically, gadolinium contrast agents used in magnetic resonance imaging (MRI) are artificial compounds that are not usually present in the body, and functional imaging similar to organ perfusion imaging can be performed by administrating these agents intravenously and obtaining their signals. However, the images thus obtained are confined only to circulation in blood vessels. Positron emission tomography (PET) can obtain

E. Shimosegawa (✉)
Graduate School of Medicine, Osaka University, Suita, Osaka, Japan
e-mail: eku@mi.med.osaka-u.ac.jp

M. Kasaki et al. (eds.), *Cognitive Neuroscience Robotics B*,
DOI 10.1007/978-4-431-54598-9_8

natural circulation through the body, from blood vessels to organs and from organs to blood vessels, as molecular images following labeling water, which is naturally present *in vivo*, with a radioisotope.

A problem in visualizing brain neuronal activity is the difficulty of comprehensively representing it, because the functions of the brain cover metaphysical areas, such as mind, consciousness and intention, and individual activities cross each other in a complicated manner, unlike in other organs. Therefore, also in PET molecular imaging with radioisotope compounds as tracers, it should be supposed that brain functions are localized, that each nerve type differentiates separately and that functional molecules come into and go out of the tissue in a quantitative manner. Furthermore, their quantity should be analyzed by collecting signals, *i.e.*, radiation released from the body, and converting them to a parameters set based on a virtual mathematical model. There are limitations in elucidating the whole picture of neurological functions by this method. However, tracers used in PET could be powerful tools in neuroimaging research, in that they are based on natural molecules constituting organisms, thereby making it possible to obtain specific molecular images of circulation, metabolism, neuroreceptor functions and activity of each cell.

This chapter describes the latest status of imaging research on neurological functions, that are mainly related to PET.

8.2 Brain Neuronal Activity and Cell-Specific Energy Metabolism

The brain is an organ with active energy metabolism, and oxygen consumption in the brain reaches approximately 20 % of the total oxygen consumption just to maintain basal metabolism. In the brain, most energy is consumed for active transport of ions involved in maintaining the neuronal membrane potential. Although the activity of brain tissue is maintained by a large amount of adenosine triphosphate (ATP) produced by oxidative phosphorylation of glucose, brain tissue has no efficient storage system such as glycogen and requires a constant supply of glucose and oxygen. If cerebral ischemia occurs due to the occlusion of cerebral blood vessels, reduced supply of glucose and oxygen to the brain induces impairment of the neuronal membrane potential, which suppresses neuronal firing and directly leads to a decrease in neurotransmission functions.

On the other hand, if brain neuronal activity increases by thinking and speaking, neuronal energy metabolism increases in the relevant local brain centers, and cerebral blood flow (CBF) also increases, leading to an increased supply of glucose and oxygen. Therefore, if the results of a relatively simple task are summarized as a certain brain function or thinking process, brain neuronal activity after receiving the task from the outside can be visualized as images of areas with an increase in CBF.

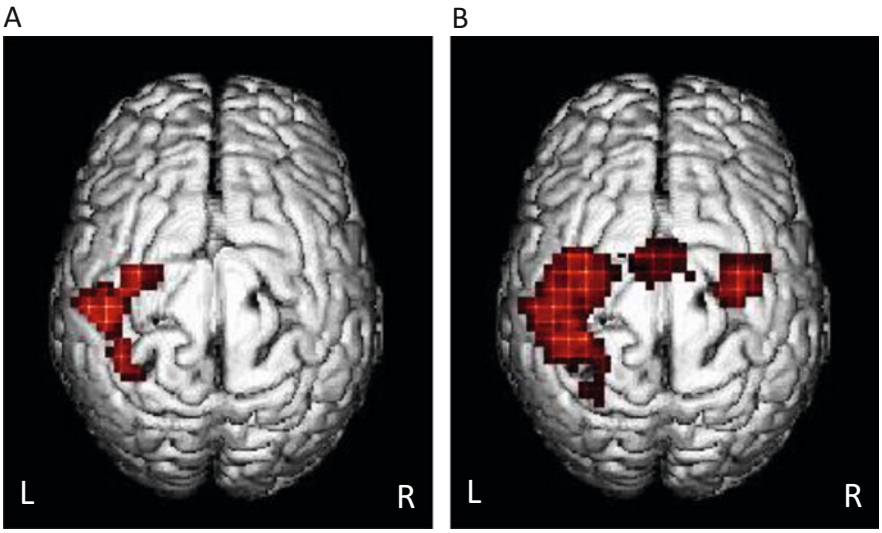

Fig. 8.1 Brain activation study with moving right hand. (**a**) Simple motor task by finger tapping. (**b**) Complex motor task by finger tapping and position changing (Courtesy Dr. Atsushi Umetsu.)

This is called localized brain activation (stimulation) study. Figure 8.1 shows the visualization of differences in locally activated brain areas in response to different tasks, a simple or somewhat complex movement, using functional magnetic resonance imaging (f-MRI), in the task of moving one hand.

Up to the present, brain energy metabolism has been studied focusing on neurons. However, in recent years, new metabolic images are being visualized from new points of view. Although it had long been considered that the only role for glial cells was as a supporting tissue of the brain, these cells were revealed to play an important role in supplying lactic acid necessary for neuronal energy metabolism. Astrocytes, which are glial cells present in the central nervous system, incorporate more than twice as much glucose as neurons do and generate lactic acid from pyruvic acid through the glycolytic pathway. Lactic acid is a compound from which acetyl coenzyme A (acetyl-CoA), an important substrate in the tricarboxylic acid (TCA) cycle, is generated, and astrocytes are a major source of supply of lactic acid necessary for neurons through the astrocyte-neuron-lactate shuttle (Dienel and Cruz 2006; Dienel and Hertz 2001) (Fig. 8.2). In addition, glutamate generated by the TCA cycle metabolism in neurons is released as a neurotransmitter from the termini of presynaptic neurons to the synaptic cleft and binds to receptors on postsynaptic neurons, and thus neurotransmission is achieved. In this process, excitatory glutamate released in excess to the synaptic cleft acts as a neurotoxin, if its concentration is high. Astrocytes are also involved in glutamate-glutamine cycling, in which excitatory glutamate in the synaptic cleft is recovered, detoxified to glutamine through gamma-aminobutyric acid (GABA) and reused in the termini

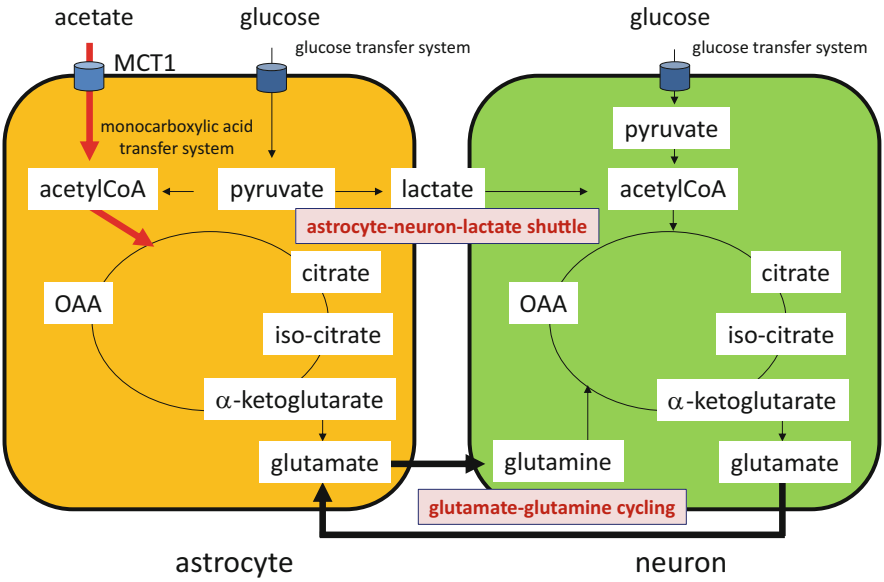

Fig. 8.2 Model for energy cycling of neuronal and glial activity with glucose utilization. *MCT1* monocarboxylic acid transporter-1, *OAA* oxaloacetate. MCT1 is a specific transporter for acetate intake into astrocyte

of presynaptic neurons (Friston et al. 1991) (Fig. 8.2). As described above, astrocytes have been revealed to play an important role in supporting neuronal energy metabolism and neurotransmission.

Energy metabolism in astrocytes can be visualized by the radioactivation of energy substrates that are specifically incorporated into astrocytes but not into neurons. Acetic acid is specifically incorporated into astrocytes via monocarboxylate transporters and contributes to the turnover of the TCA cycle. Carboxylic acid in this compound can be radiolabeled with ^{11}C to prepare a PET agent. Figure 8.3 shows a normal brain PET image using ^{11}C-acetic acid, in which glial cell-specific energy metabolism was visualized. Hertz et al. visualized changes in acetate metabolic activity in rats given auditory stimulation using ^{14}C-labled acetic acid, compared them with areas where glucose metabolism was activated and proved that these metabolisms increase in the same areas (Heiss et al. 2004).

It has not been elucidated yet how the brain obtains and consumes energy required for higher brain function activity or how differences in activity among central nervous system cell types affect higher brain function. Research on energy metabolism imaging using PET may provide new clues in this field.

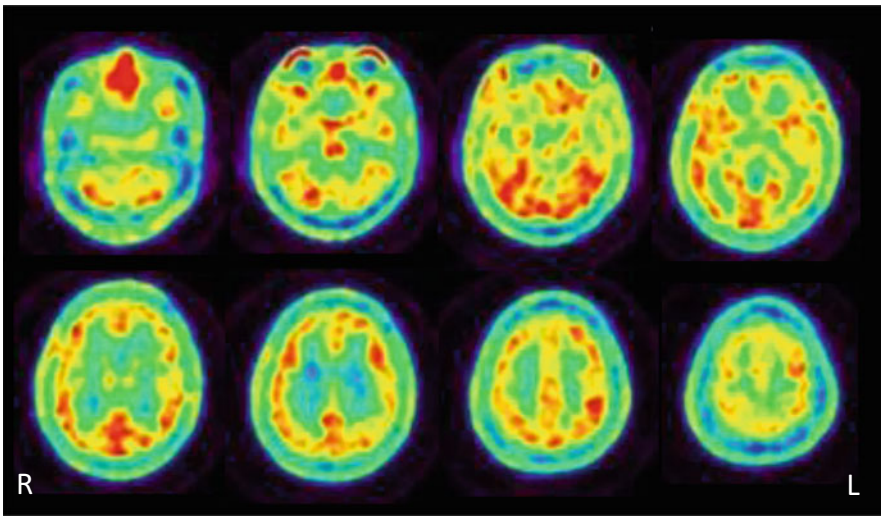

Fig. 8.3 ^{11}C-acetate brain distribution in a healthy volunteer measured by PET

8.3 Cognitive Impairment and Neuroimmunity

Population aging has advanced, and early detection of pathological cognitive impairment attracts high attention. Alzheimer's disease is a representative disease, and according to a famous hypothesis explaining its development, aggregation and accumulation of amyloid protein (Aβ) due to the cleavage of amyloid precursor protein (Fig. 8.4) and neurofibrillary tangles due to the expression and phosphorylation of the tau protein occur in a cascade fashion (Hertz et al. 2007). It is clinically important to establish an early screening system for middle-aged and elderly patients who have developed mild cognitive impairment (MCI) within the allowable range as a normal age-related change to assess the potential future development of Alzheimer's disease, to provide them with treatment and to improve their quality of life through enhanced activities of daily living.

Studies using PET employ procedures in which compounds that specifically bind to aggregated Aβ are labeled to perform imaging, and many agents have been developed, represented by [^{11}C]Pittsburgh compound B (^{11}C-PIB), [^{11}C]2-(2-[2-dimethylaminothiazol-5-yl]ethenyl)-6-(2-[fluoro]ethoxy)benzoxazole (^{11}C-BF227), 2-(1-6-[(2-[^{18}F]fluoroethyl)(methyl)amino]-2-naphthylethylidene) malononitrile (^{18}F-FDDNP), ^{18}F-BAY 1008472 and ^{11}C-AZD2995. In particular, ^{11}C-PIB, which was developed in the early days, was tested in a large-scale international clinical trial, and it was reported that patients with low accumulation of ^{11}C-PIB in the brain did not develop Alzheimer's disease (Kato et al. 2008). However, its specificity for predicting conversion to Alzheimer disease is low in MCI patients with ^{11}C-PIB accumulation. In addition, its accumulation is low in disease types other than Alzheimer's disease, such as frontotemporal dementia, and

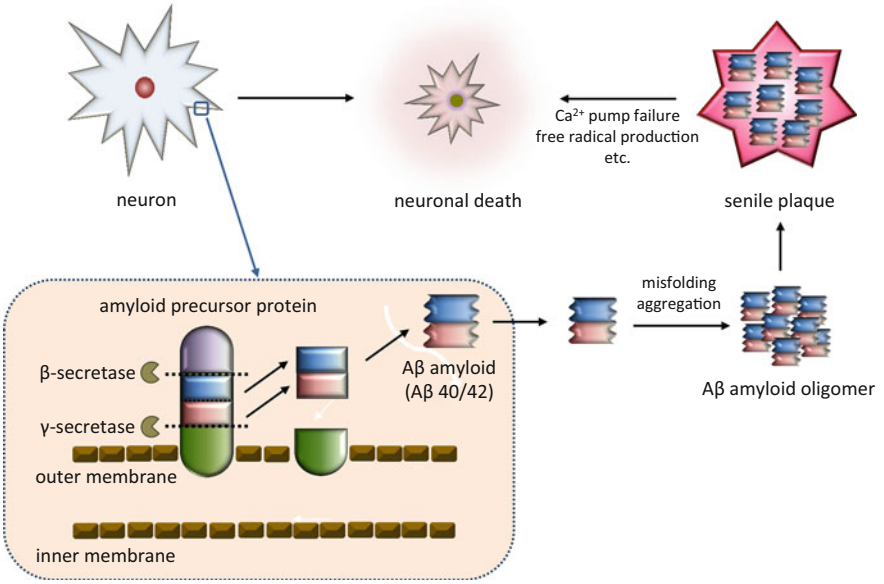

Fig. 8.4 Schema of senile plaque formation based amyloid hypothesis in Alzheimer's disease

it is also difficult to differentiate between such disease types and normal conditions. Therefore, agents that bind to abnormally accumulated substances in the brain with higher pathological specificity, such as the tau protein, are being searched for. Furthermore, new PET agents are being developed for diseases that have molecular pathologically distinct accumulated substances, such as α-synuclein and TAR DNA-binding protein 43 (TDP-43), and are also pathologically distinguished from Alzheimer's disease, such as Parkinson's disease and frontotemporal dementia.

Attention has not often been paid up till now to immune reactions in the field of neuroscience. However, it was recently observed that activated microglia induce immune responses against aggregated Aβ leading to neuroinflammation, in the pathogenesis of Alzheimer's disease (Matsuda et al. 2007). It is now possible to perform imaging of abnormally expressed activated microglia using a PET agent prepared by labeling a protein that binds to receptors on the mitochondrial outer membrane of activated microglial cells.

8.4 Improvement in Resolution and Sensitivity of PET Devices

There are several points that should be kept in mind when localized brain activation studies are conducted using PET. One is that, because of the influence of the positron range and internal absorption/scattering of radiation, PET images have poor spatial resolution compared to MRI and CT images, making it difficult to identify anatomical sites, and it takes time to collect data. To overcome these disadvantages, devices with highly sensitive detectors and new data collection methods have been developed. Detectors can be thinned and high-resolution images can be obtained by adopting semiconductors in detectors (Fig. 8.5). Local brain anatomy can also be identified in small animal imaging by using semiconductor PET devices (Fig. 8.6). In addition, sensitivity in the detection of radioactive concentration has improved and data acquisition time and exposure dose can be reduced by the three-dimensional data collection of radiation generated in the field of view of devices (Fig. 8.7). The development of the above latest devices has made it possible to analyze the energy metabolism in small structure of the brain, which could not have been visualized by the conventional PET scanner. In particular, the brainstem contains many nuclei from which various nervous systems originate, but has not been studied in the field of higher brain function activity. High glucose metabolic activity can be visualized in areas where there are aggregates of brain

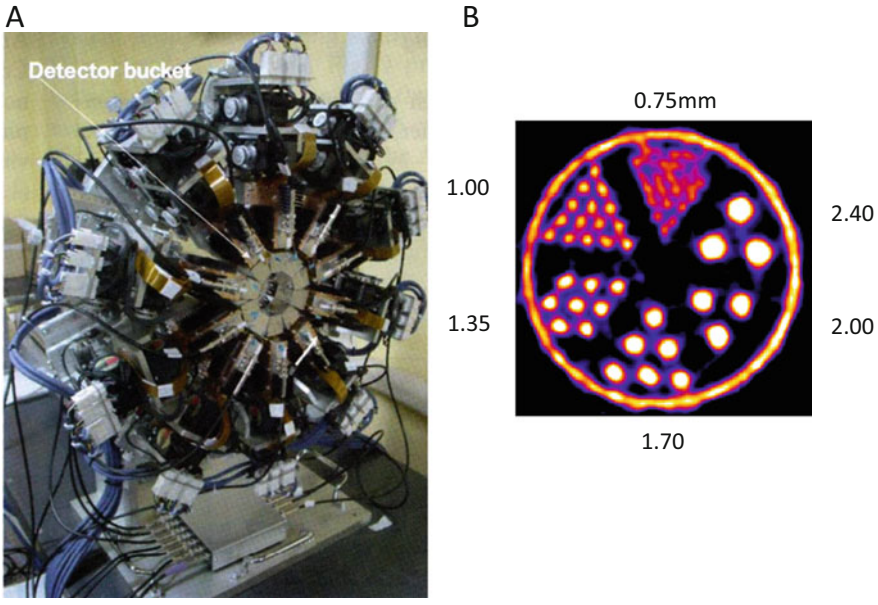

Fig. 8.5 High resolution and high sensitivity PET system made by semiconductor detectors. (**a**) A semiconductor PET system without gantry cover. (**b**) Images of the Derenzo phantom obtained by a semiconductor PET. Axial spatial resolution of this PET system is 1.00 mm

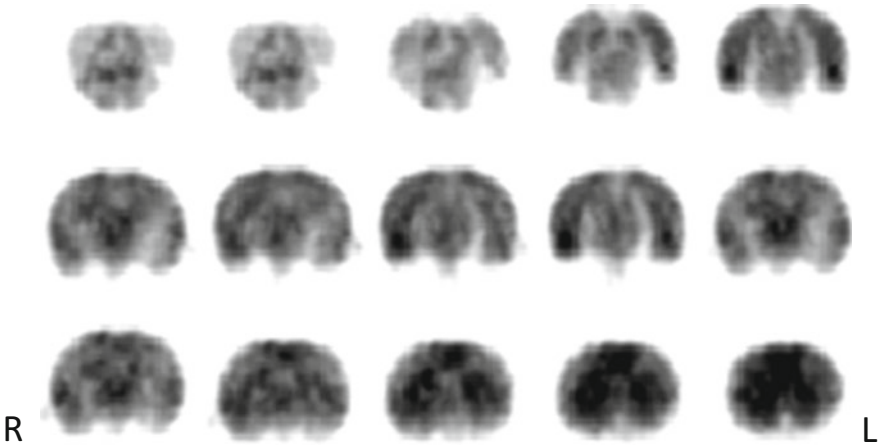

Fig. 8.6 Quantitative image of cerebral metabolic rate of glucose utilization in a normal rat measured by a high-resolution semiconductor PET system

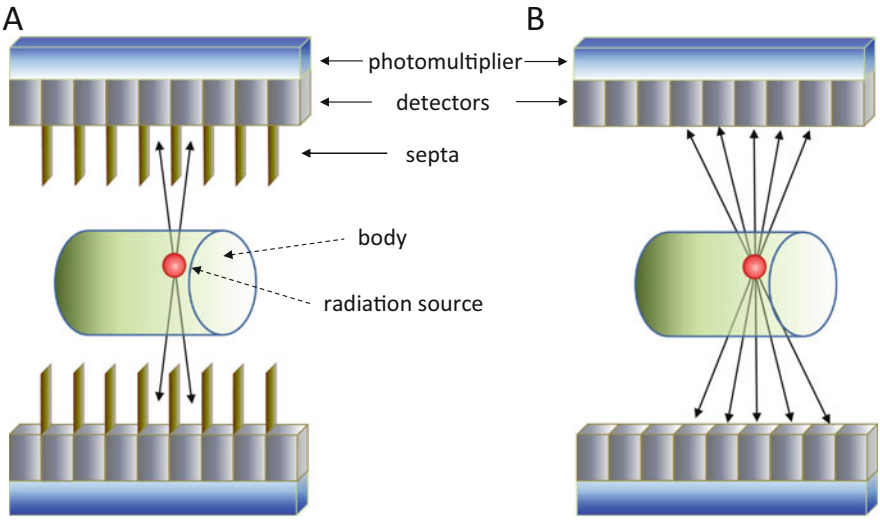

Fig. 8.7 Schema of data collection of 2-dimensional (2-D) and 3-dimensional (3-D) PET system. (**a**) 2-D PET has septa between each detector to eliminate scatter radiation. (**b**) 3-D PET system has high image sensitivity because it can collect many radiations from the radiation source without being disturbed by septa

nuclei, such as the brainstem reticular formation involved in consciousness and perception, by using high-resolution and high-sensitivity PET devices (Minoshima et al. 1995) (Fig. 8.8). Interrelation and differences in activity between these

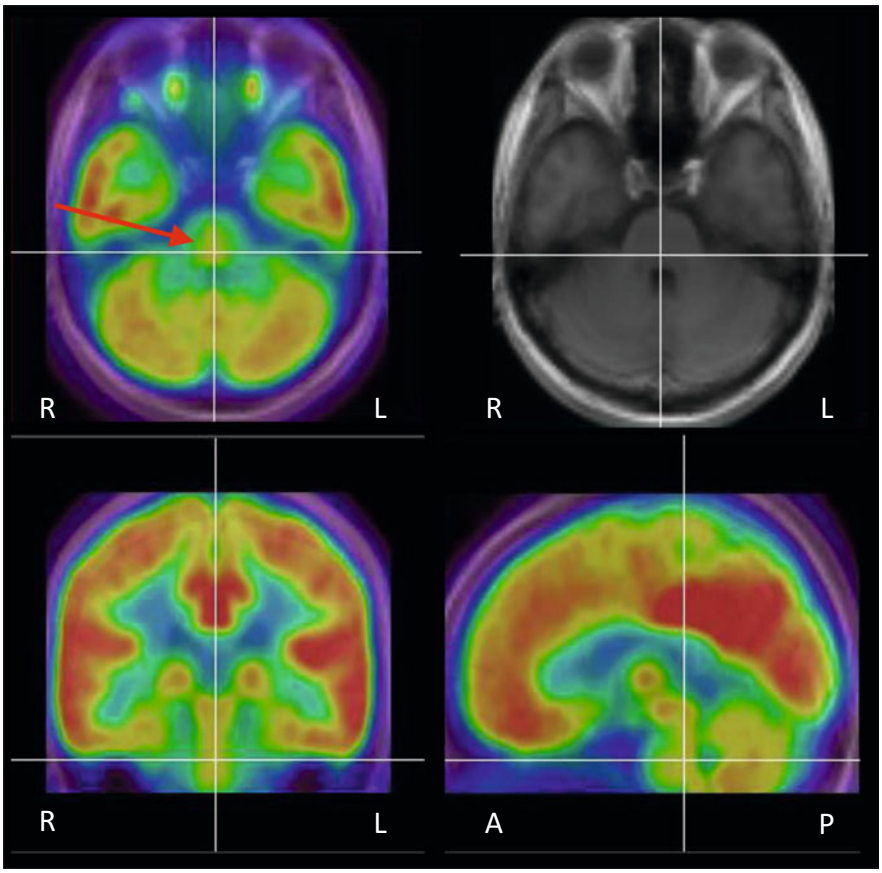

Fig. 8.8 Normal brainstem glucose metabolism measured by ^{18}F-FDG PET. Averaged PET image of healthy volunteers (*upper left*) shows high glucose metabolism in the dorsal area of the pons (*red arrow*), corresponding to the brainstem reticular formation

brainstem nuclei and the cerebral neocortex are unexplored fields in localized brain activation studies.

8.5 Automated Image Analysis and Its Statistical Evaluation

Methods conventionally used for analysis of PET images are visual evaluation and analysis with a regions-of-interest (ROI) setting. Visual evaluation, however, does not allow quantitative analysis, thus making it impossible for PET image readers to

enjoy the advantage of analyzing the linear relationship between biofunctions and radioactivity level. Analysis with the ROI setting involves the step of setting an ROI of any form in freely selected regions of the image and the step of quantitatively measuring the radioactivity level in the pixels within the ROI. Problems with this approach lay in that the selection of the place and size of the ROI is affected by arbitrary elements and that it is difficult to set an ROI covering the entire brain.

In recent years, statistical image analysis has been advancing as a means allowing the simple and objective analysis of images. A representative method of this category is Statistical Parametric Mapping (SPM) devised by Friston et al. as a method of inter-group comparison (Okello et al. 2009). In the field of medicine, the neurologic statistical image analysis program (NEUROSSTAT; University of Washington) and the easy Z-scores imaging system (e-ZIS; Fiji Film RI Pharma Co.) are used extensively as techniques for comparison between group (healthy group or sick group) and individuals (Pellerin et al. 2007; Talairach and Tournoux 1988).

With basic methods of statistical image analysis such as SPM, measurement is done on the PET images collected from the subjects to be compared, and the continuous probability distribution of brain tissue radioactivity level in each pixel is determined and fed into a database. From the continuous probability distribution data for each pixel from each group collected in this manner, pixels with a statistically significant elevation or reduction of probability are extracted from each group and depicted as a map of the statistical values of the pixels concerned on brain images. With this method, several steps of image processing are needed before the statistical analysis. First, the brain images of varying forms from individual subjects must undergo linear or nonlinear transformation and are fit into a single template, i.e., the standard brain (anatomical normalization). Through this step, the pixels constituting the brain images of subjects are all located on the same axis of the coordinate within the three-dimensional visual space. Next, the radioactivity levels are standardized by setting of a threshold level for the radioactivity level of individual pixels or dividing the radioactivity level in individual pixels by the whole brain radioactivity level or the radioactivity in a reference area. Subsequently, using a prescribed statistical method, the continuous probability distribution of individual pixels is compared between groups, to extract pixels with significant inter-group differences. The pixels extracted following this procedure are developed on the Talairach brain atlas (Tanzi and Bertram 2005) or the standard brain image, to identify the anatomical site concerned (Fig. 8.9). In addition to these steps, some other steps such as realignment and smoothing are incorporated into this method to reduce statistical noise from the images.

Several requirements need to be satisfied to enable adoption of this analytical method. First, the brain of the subject to be analyzed must be free of marked deformation, defect or atrophy as compared to the standard brain. If the brain form differs markedly from that of the standard brain, pixel dislocation may occur during the process of anatomical normalization, and an accurate analysis is not possible due to an admixture with the radioactivity in tissue other than the target site. Furthermore, to

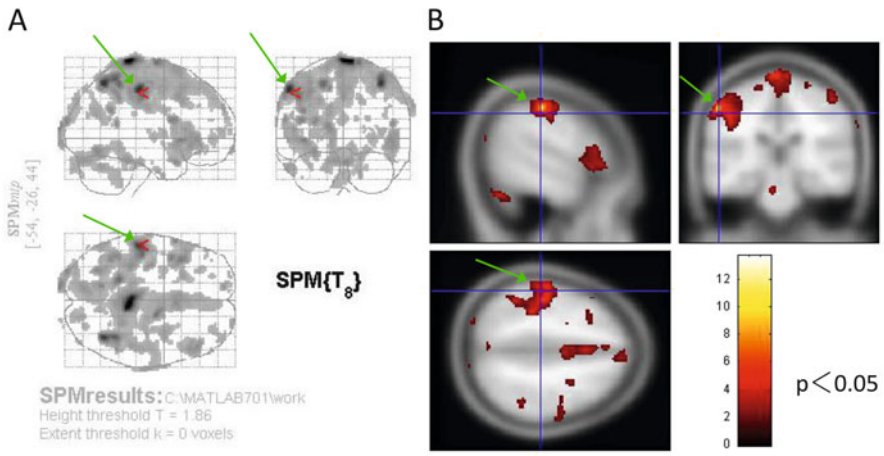

Fig. 8.9 Image analysis for the CBF difference between normal male and female using statistical parametric mapping (SPM). (**a**) Areas with significantly higher CBF in female than in male demonstrated on the Talairach atlas. Coordinate-54, -26, and 44 (*green arrow*) corresponded to the Brodmann area 2 (postcentral gyrus). (**b**) Overlayed image on three intersecting (sagittal, coronal, transaxial) slices of MRI-T_1 template image

enable automated anatomical normalization, it is necessary to use a PET agent whose radioactivity can be distributed extensively within the brain, like the distribution on brain perfusion images or brain glucose metabolism images. In addition, all subjects covered by a single analysis need to undergo imaging with the same PET device combined with the same PET agent, followed by image reconstruction with the same technique. This is necessary because different PET agents have different characteristics in local brain distribution and because the image quality can be altered by the method of image collection or reconstruction, causing statistical noise. Regarding the composition of the groups of subjects, it is necessary to cover a large population so that the precision of the statistical detective power can be improved, and it is also necessary to ensure uniformity of all groups in terms of background elements (e.g. age group and gender) possibly affecting the analytical results.

In any event, statistical image analysis is a noninvasive method for objective evaluation of radioactivity distribution, not necessitating measurement of the input function by arterial blood sampling (needed for quantitative test) but enabling simple analysis if data from a reliable database are collected with the same device and the same method. SPM is a computer program of the "freeware" category (http://www.fil.ion.ucl.ac.uk/spm/) which has been used extensively not only for PET image analysis but also for analysis of functional MRI data in regional brain activation testing. In addition, this program can be used for interim processes (anatomical normalization, smoothing, etc.) in its unique way. Because of these

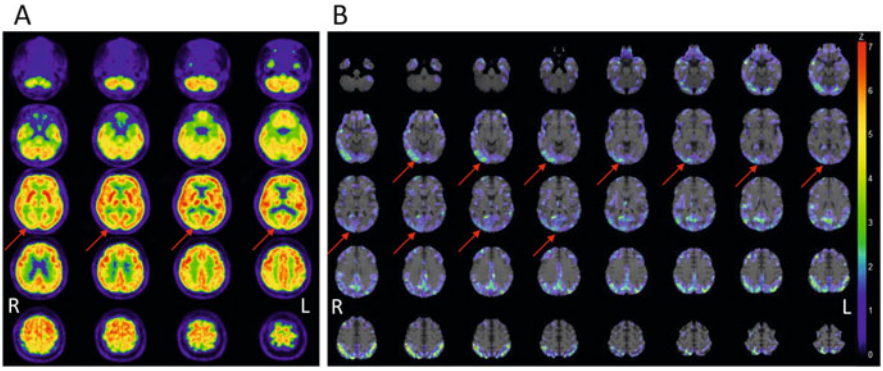

Fig. 8.10 Statistical image analysis of the brain glucose metabolism in a patient with probable diffuse Lewy body disease. (**a**) Original ^{18}F-FDG-PET images showed subtle decrease of glucose metabolism in the right primary visual cortex (*red arrow*). (**b**) Statistical image analysis by NEUROSTAT software demonstrated areas with significantly decrease of glucose metabolism compared with normal database

features, the program has been applied to diverse studies involving images. NEUROSTAT and e-ZIS, which enable group vs. individual comparison, are often used for identification of brain sites with reduced perfusion or glucose metabolism through neuronal degeneration in the diagnosis of dementia and for disease typing, thus providing a useful tool in clinical medicine (Fig. 8.10). They are also used for the analysis of neuroreceptor images to identify the epileptic focus.

8.6 Integration of Different Imaging Devices and Advances in Small Animal Imaging

To improve the diagnostic ability of PET imaging with poor spatial resolution, PET/CT devices in which PET and CT are combined are currently generally used (Fig. 8.11). The acquisition of CT images before and after acquisition of PET images and fusion of these images using an integrated CT-PET device have made it possible to more clearly identify the visual biodistribution of radioisotope compounds (Fig. 8.12). In addition, the measurement of the internal permeability of X-ray from the outside using a CT device has also made it possible to estimate the internal absorption of radioactivity to correct measured values obtained with a PET device.

Devices involving combinations of different technologies, as described above, represent a major trend in the development of the latest devices. In recent years, attention has also been paid to the combination of PET and MR devices, and devices offering practical indications in the clinical field are now commercially

Fig. 8.11 Integrated PET/CT scanner for clinical measurement. The scanner can collect radiations from field-of-view with 3-D data acquisition system, which can reduce radiation dose without disturbing image quality

available. Particularly in the field of neuroscience, studies using integrated PET/MR devices are prospective. In higher brain function tests, it is possible to simultaneously collect the distribution of various radioactive tracers using PET and functional images, such as MRI tractography and functional MRI images, and to compare them. In addition, PET images with low resolution have to be normalized to the anatomical standard brain by software processing after higher brain function tests, and activated areas of local brain function have to be evaluated in comparison with the brain atlas. However, simultaneous acquisition of PET and MR images in the same subjects using PET/MR devices makes it easier to evaluate active areas in the deformed brain due to developmental abnormalities and in the pathologically damaged brain that cannot be processed by software. Furthermore, a method has been devised to correct the underestimation of radioactivity due to the presence of tissues other than the brain, air, etc. in image voxels (partial volume effect) by collecting PET and MR images simultaneously (Villemagne et al. 2011) (Fig. 8.13).

The combination of PET and MR devices also greatly benefits small animal imaging (Fig. 8.14). Naturally, it is even more difficult to anatomically evaluate radioactivity distribution in the imaging of small animals using PET with poor resolution, but the fusion of PET and MRI, the latter of which has excellent density resolution, makes it easier to analyze radioactivity distribution in organs such as the

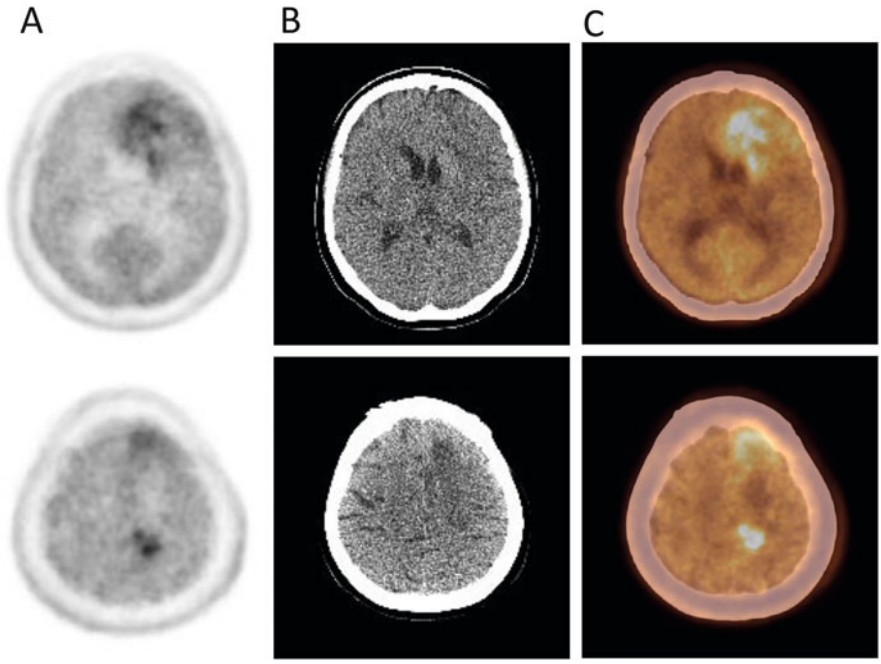

Fig. 8.12 Diagnostic utility of fused image between PET and CT in a patient with glioblastoma. (**a**) ^{11}C-methionine PET image (amino acid tracer) for the detection of tumor infiltration in the brain, (**b**) CT image at the same level of ^{11}C-methionine PET obtained by integrated PET/CT system, and (**c**) fused image between PET and CT. Functional brain damage examined by PET can be clearly identified by morphological information by CT

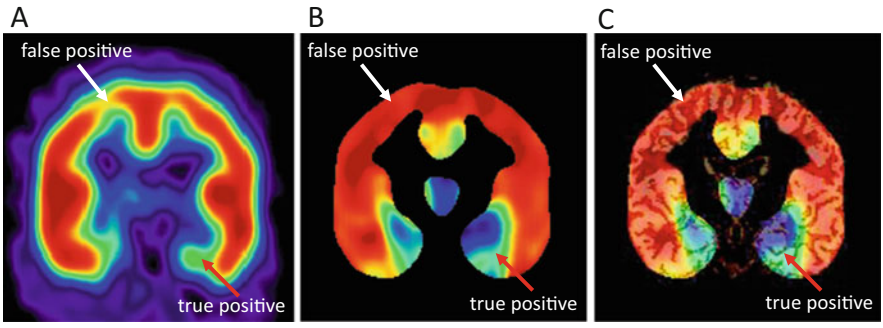

Fig. 8.13 Improvement of diagnosis in a patient with epilepsy by partial volume effect (PVE) correction. (**a**) Uncorrected PET or single photon computed tomography (SPECT) image, (**b**) PVE-corrected PET or SPECT image, and (**c**) fused image between PVE-corrected image and gray matter MRI map. False positive are (*white arrow*) and true positive are (*red arrow*) precisely diagnosed by the PVE-corrected image

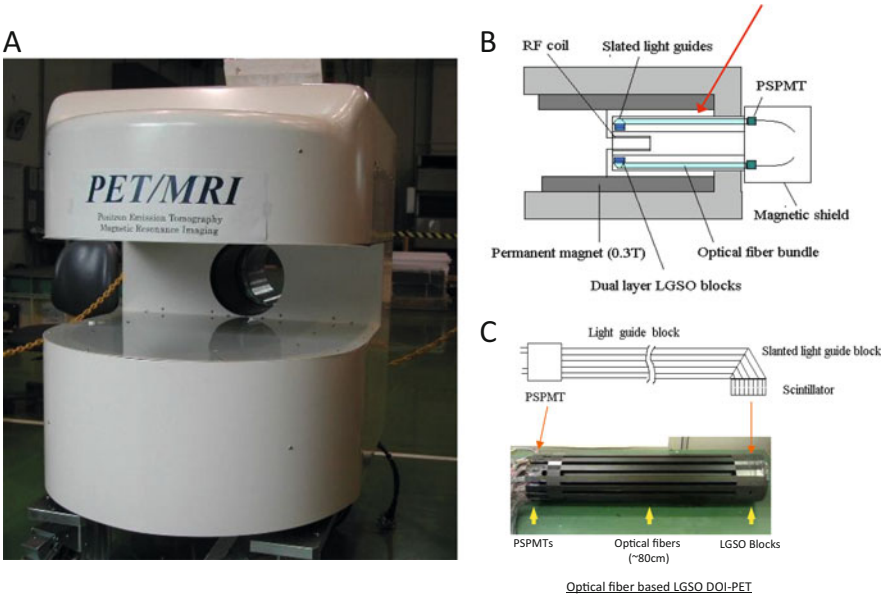

Fig. 8.14 (**a**) Appearance of an integrated PET/MRI scanner for animal experiment, (**b**) its vertically-sectioned diagram, and (**c**) the detector system in PET portion. The scanner combined PET portion with an open-type MRI portion with a 0.3 T permanent magnet. The PET portion (*red arrow*), consisted of detectors and optical fibers, which was placed between the radiofrequency (RF) coil and permanent magnet for MRI. Position-sensitive photo-multiplier tubes (PSPMT), covered with magnetic shield, are located behind the yoke

brain and spinal cord (Fig. 8.15). In addition, in pathological studies of cerebrovascular disease, such as those using transient cerebral ischemia models, brain functional images and the state of cerebrovascular occlusion and recanalization can be examined by simultaneously obtaining cerebral blood flow and metabolic images using PET and magnetic resonance angiography (MRA) images. Although a large number of animals have been used so far in such studies, and autopsied to obtain ideal experimental models, based on these results leading to the subsequent development of innovative combined technology systems, such tasks can now be replaced by the in vivo imaging of a small number of animals. The development of the above-described innovative experimental devices has made it possible to obtain molecular images in living animals using protocols similar to those used for humans.

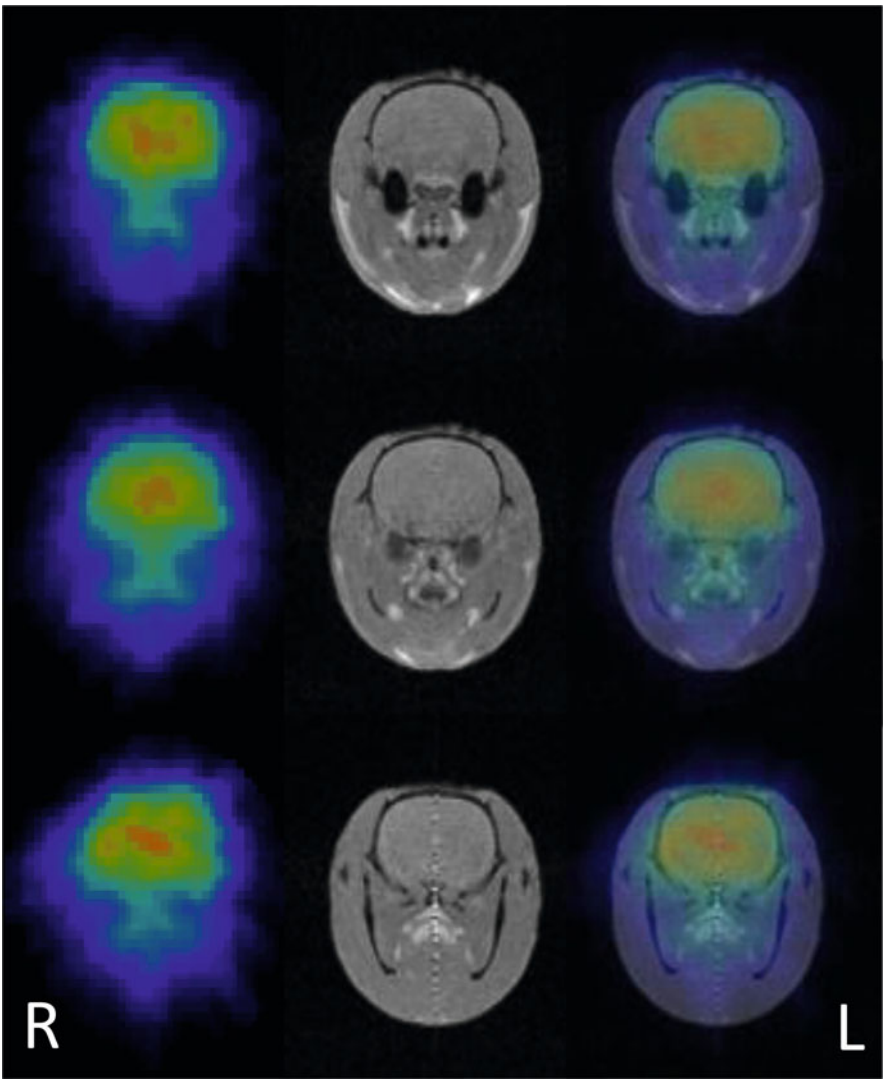

Fig. 8.15 Image fusion between PET and MRI in a normal rat obtained by the integrated PET/MR scanner. ^{18}F-FDG PET image (*left column*), MRI (*middle column*), and fused PET and MR image (*left column*)

8.7 Concluding Remarks

The brain is an organ that controls the total organism, including what is referred to as the mind. Although various means, including PET, have been devised to observe the activities and movement of the mind from the outside, it is difficult to comprehensively investigate its profound areas. However, organisms are consisted of

molecules, and if the functions and activities of the brain can be converted to signals, digitized and analyzed as molecular actions, it is possible to perform their imaging. Although PET has limitations, such as spatial resolution, radiation exposure and limited observation periods due to short half-life isotopes, efforts are being continuously made to elucidate more minute brain functions by introducing new radiopharmaceuticals, developing devices, improving imaging techniques and innovating analytical procedures.

Exercise

What significance do the fusion of a functional image and the morphological image have for neurologic image analysis?

References

Dienel, G.A., Cruz, N.F.: Astrocyte activation in working brain: energy supplied by minor substrates. Neurochem. Int. **48**, 586–595 (2006)

Dienel, G.A., Hertz, L.: Glucose and lactate metabolism during brain activation. J. Neurosci. Res. **66**, 824–838 (2001)

Friston, K.J., Frith, C.D., Liddle, P.F., et al.: Comparing functional (PET) images: the assessment of significant change. J. Cereb. Blood Flow Metab. **11**, 690–699 (1991)

Heiss, W.D., Habedank, B., Klein, J.C., et al.: Metabolic rates in small brain nuclei determined by high-resolution PET. J. Nucl. Med. **45**, 1811–1815 (2004)

Hertz, L., Peng, L., Dienel, G.A.: Energy metabolism in astrocytes: high rate of oxidative metabolism and spatiotemporal dependence on glycolysis/glycogenolysis. J. Cereb. Blood Flow Metab. **27**, 219–249 (2007)

Kato, H., Shimosegawa, E., Oku, N., et al.: MRI-based correction for partial-volume effect improves detectability of intractable epileptogenic foci on ^{123}I-iomazenil brain SPECT images. J. Nucl. Med. **49**, 383–389 (2008)

Matsuda, H., Mizumura, S., Nagao, T., et al.: Automated discrimination between very early Alzheimer disease and controls using an easy Z-score imaging system for multicenter brain perfusion single-photon emission tomography. Am. J. Neuroradiol. **28**, 731–736 (2007)

Minoshima, S., Frey, K.A., Koeppe, R.A., et al.: A diagnostic approach in Alzheimer's disease using three-dimensional stereotactic surface projections of fluorine-18-FDG PET. J. Nucl. Med. **36**, 1238–1248 (1995)

Okello, A., Edison, P., Archer, H.A., et al.: Microglial activation and amyloid deposition in mild cognitive impairment: a PET study. Neurology **72**, 56–62 (2009)

Pellerin, L., Bouzier-Sore, A.K., Aubert, A., Serres, S., Merle, M., Costalat, R., Magistretti, P.J.: Activity-dependent regulation of energy metabolism by astrocytes: an update. Glia **55**, 1251–1262 (2007)

Talairach, J., Tournoux, P.: Co-Planar Stereotactic Atlas of the Human Brain. Theime Verlag, Stuttgart (1988)

Tanzi, R.E., Bertram, L.: Twenty years of the Alzheimer's disease amyloid hypothesis: a genetic perspective. Cell **120**, 545–555 (2005)

Villemagne, V.L., Pike, K.E., Chételat, G., et al.: Longitudinal assessment of Aβ and cognition in aging and Alzheimer disease. Ann. Neurol. **69**, 181–192 (2011)